

END OF LIFE DISPOSAL OF SATELLITES IN THE GEO REGION, THE ISSUE OF HIGH INCLINATIONS

Vincent Morand⁽¹⁾, Hubert Fraysse⁽²⁾, Alain Lamy⁽²⁾, Clémence Le Fevre⁽²⁾ and Romain Pinede⁽³⁾

⁽¹⁾⁽²⁾ CNES, 18 av. Edouard Belin 31401 Toulouse Cedex 9, FRANCE, vincent.morand@cnes.fr

⁽³⁾ THALES, SIX/CIS/SSE Toulouse, France, romain.pinede@thalesgroup.com

Abstract: An international consensus states that after their end of mission space objects within the GEO protected region have to be moved to disposal orbits that ensure the non-crossing of the protected region within the next 100 years. The choice of the disposal orbit is relatively simple for typical geostationary satellites due to the smooth perturbations that affect their orbits. However, the disposal of space objects in geosynchronous orbits, i.e. at the geostationary altitude but with non-zero inclinations, is more tedious, especially in the case of high inclinations. Extreme eccentricity variations happen, making the disposal orbit to cross the protected area. The paper will explain the physical phenomena leading to those variations: the resonance conditions will be analyzed to try to identify a critical orbit domain. Then, the selection of an appropriate disposal orbit for space objects initially found in such a critical orbit domain will be discussed.

Keywords: orbit propagation, end of life disposal, GEO protected region, resonances

1. Introduction

Since the launch in 1963 of Syncom2, the first successful geosynchronous satellite, geosynchronous orbits (GSO) have been extensively used, mainly for communications purposes. The UCS satellite database [1] refers about 450 operational satellites in GSO, two third of them for commercial purpose and the last third being referred as “Military” or “Government”. About 1400 satellites (both operational and non-operational) are catalogued in GSO [2]: Fig. 1 shows their repartition. Most of them are in geostationary orbit (GEO), but a few of them lies on orbits at “high inclinations” (Military satellites or part of the Compass constellation).

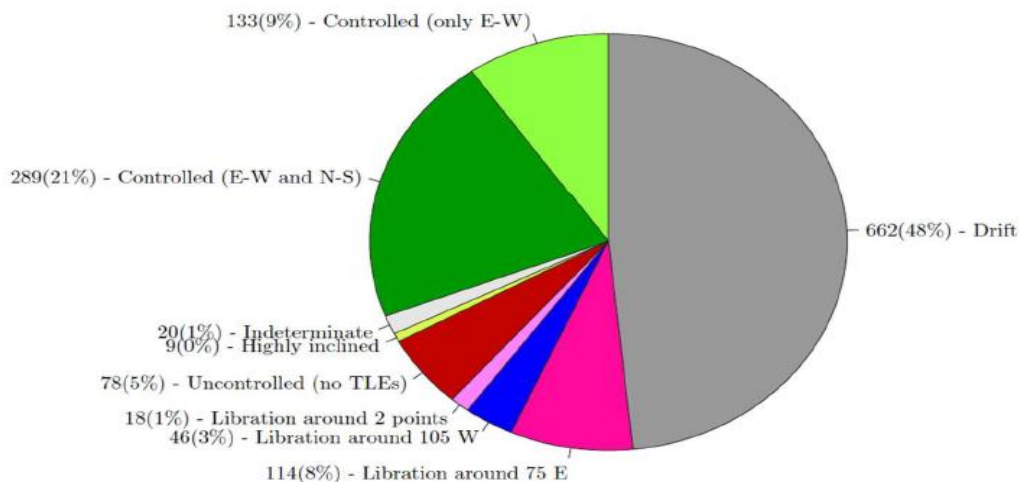


Figure 1: GEO satellite repartition (from [2])

The need of a clean disposal of space objects orbiting near the GEO altitude is shared among space agencies. The Inter Agency Space Debris Coordination Committee (IADC) defined the protected region B: altitude between GEO – 200km and GEO + 200km; latitude between -15 deg and +15 deg (the protected region A concerns Low Earth Orbits).

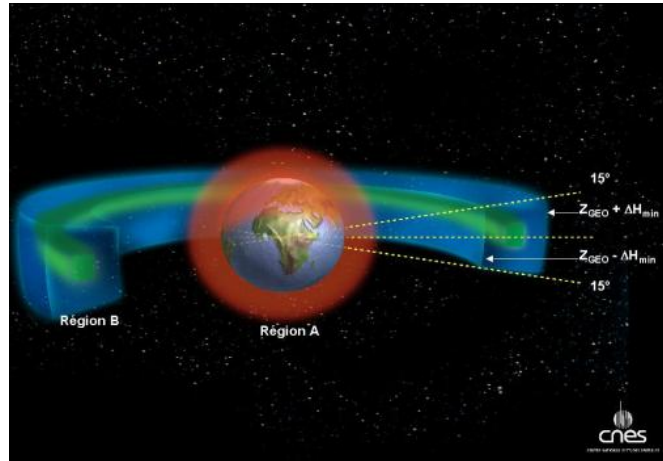


Figure 2 : IADC protected region

After their end of mission, space objects within the GEO protected region have to be placed on disposal orbits that ensure the non-crossing of the protected region within the next 100 years. The so-called “ISO formula” [3] is often used to compute the minimum disposal orbit perigee altitude ΔH above the geostationary altitude that ensures compliance:

$$\Delta H = 235 + 1000 \cdot Cr \cdot \frac{A}{m} \quad (1)$$

With ΔH expressed in km, Cr the reflectivity coefficient, A the spacecraft cross sectional area and m the spacecraft mass.

In France, the French Space Operations Act (FSOA) that came into force in 2010 follows the IADC recommendations for GEO satellite disposal. Good practices have been established and a dedicated software, STELA (Semi-Analytical Tool for End of Life Analysis), has been developed to check the compliance of disposal orbits against the technical regulations attached to the FSOA [4]. At an international level, one can notice an improvement in the global rate of compliance of GEO satellites disposals with respect to the IADC recommendations, as shown in Fig.3 coming from Ref. [2]:

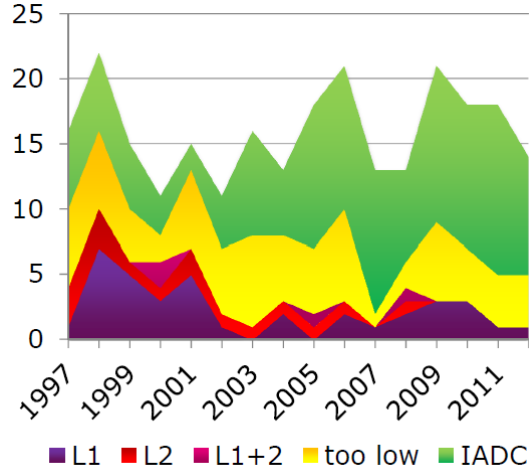


Figure 3: GEO disposal statistics

2. The issue of high inclinations: illustrations

In this chapter, we are going to present propagation results to illustrate the strong eccentricities variations noticed for GSO with “high” initial inclinations. Let us introduce the inclination vector

$$\begin{cases} ix = i. \cos(\Omega) \\ iy = i. \sin(\Omega) \end{cases} \quad (2)$$

With i the orbit inclination and Ω the Right Ascension of Ascending Node (RAAN).

In our test cases the initial inclination and RAAN will vary so that the initial inclination vector scans all its domain of definition (inclination in $[0^\circ, 180^\circ]$). Parameters of test case 1 are given in Tab.1:

Table 1 : Test case 1 parameters

Initial date	2000-03-21
Semi major axis	42464 km (GEO + 300 km)
Eccentricity	0
Inclination	Variable from 0° to 178°
Right Ascension of Ascending Node	Variable from 0° to 360°
Force model	Earth potential (7x7 model), Sun potential, Moon potential.
Propagation time	100 years
Propagation method	Semi-analytical (STELA)

One can notice that Solar Radiation Pressure is not considered in test case 1. We will demonstrate that it is not the dominant perturbation for the orbits we are interested in. Test case 1 represents more than 25,000 propagations over 100 years: it justifies the use of a semi-analytical method that is much more efficient from a computation time point of view (about one minute for 100 years of propagation). STELA software has been used. The equations implemented in

STELA are written in a set of equinoctial elements (which are not those in Eq. 2) and are valid for low and high inclinations and eccentricities. STELA has been validated by comparison with results coming from numerical propagation of a full dynamical model [5].

First, we plot the maximum inclination variations during the propagation (which is the difference between the maximum inclination and the minimum inclination) as a function of the initial inclination vector (the big circle is the domain of definition of the inclination vector).

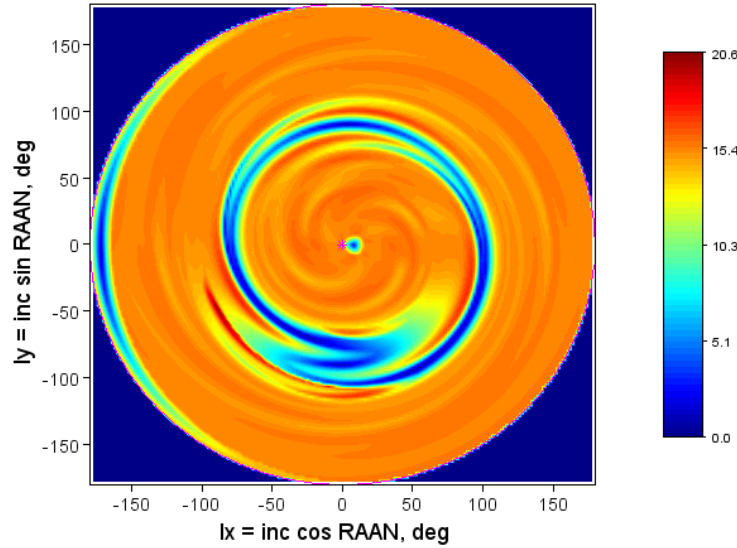


Figure 4: Maximum inclination variation (deg) vs. initial inclination vector

Fig.4 shows some classic results for GEO, such as the existence of a “stable point” for the inclination vector near $\{8, 0\}$ or the variation of about 15 degrees for an initially equatorial disposal orbit. The behavior for higher inclinations, with strong influence of the initial RAAN, is more tedious and will be explained in chapter 3. Note that the results for inclinations near 180° will not be considered since they illustrate the limitation of the set of orbital elements that makes the equations singular for $i=180^\circ$.

Then, we plot the maximum eccentricity reached during the propagation as a function of the initial inclination (left plot) or initial inclination vector (right plot)

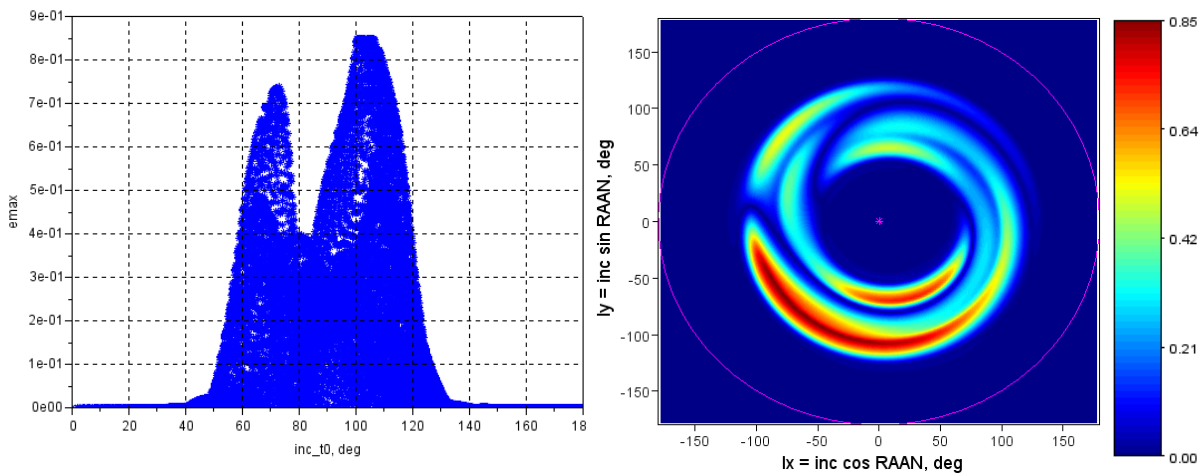


Figure 5 : Maximum eccentricity vs. initial inclination

One can see from Fig. 5 that for the initial inclinations between 50° and 130° the maximum eccentricity is higher than 0.05. Since the semi major axis is 42464 km (GEO +300km); an eccentricity of 0.0025 is big enough to bring the perigee altitude in the altitude range GEO+/- 200 km. Some of the propagations even encountered an atmospheric reentry ($e=0.85$)! The eccentricity evolutions will be explained in chapter 3.

Finally, to illustrate the chaotic behavior of the propagations in a certain range of inclinations, we computed the Mean Exponential Growth factor for Nearby Orbits (MEGNO) indicator [6]. MEGNO is a chaos indicator, whose value tends to 2 if the system is stable and to a higher value if the system is chaotic. MEGNO has been computed for each case using the transition matrix computed by STELA during the propagation [7]. For a better representation, MEGNO values higher than 3 are bound to 3 in Fig.6:

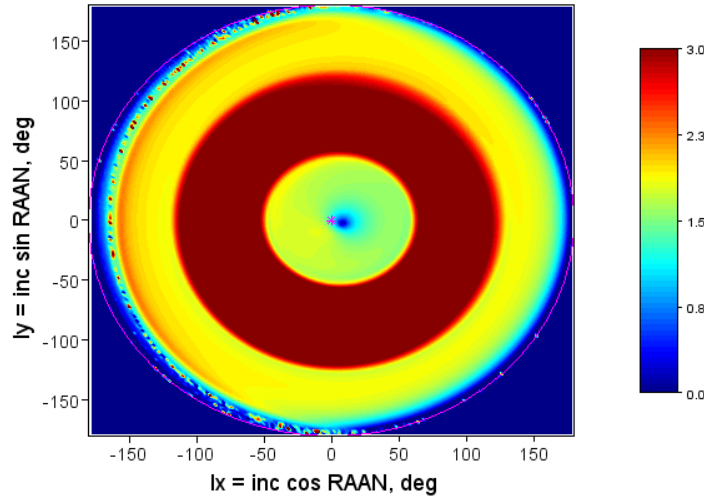


Figure 6: MEGNO indicator (bound to 3) vs. initial inclination vector

MEGNO indicator detects quite well the equilibrium point as well as the chaotic behavior for a range of inclinations.

Parameters of test case 2 are given in Tab.2:

Table 2 : Test case 2 parameters

Initial date	2000-03-21
Semi major axis	42364 km (GEO + 200 km)
Eccentricity	0
Inclination	Variable from 0° to 178°
Right Ascension of Ascending Node	Variable from 0° to 360°
Area to mass ratio	$0.1 \text{ m}^2/\text{kg}$
Force model	Earth potential (7x7 model), Sun potential, Moon potential. Solar Radiation Pressure
Propagation time	100 years
Propagation method	Semi-analytical (STELA)

The main difference between test case 2 and 1 is that we take into account the Solar Radiation Pressure, with an area to mass ratio that is quite high with respect to classic values for non-operational GEO satellites (the High Area to Mass Ratio objects discovered in GEO region will not be considered here).

Again, we plot the maximum inclination variation and eccentricity as a function of the initial inclination vector

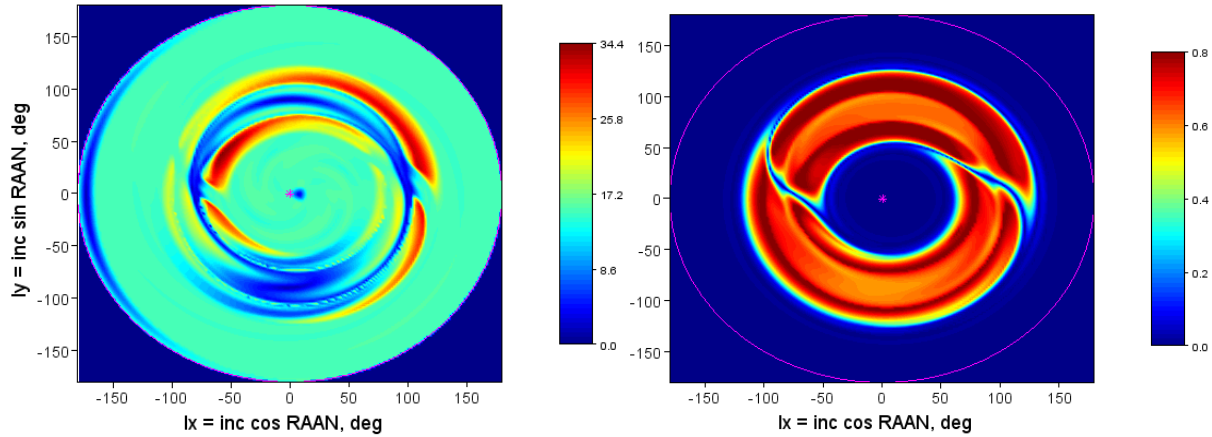


Figure 7: Maximum inclination variation (left) and maximum eccentricity (right)

We see that the main effect, coming from the 3rd body perturbation, is still present and that SRP “makes it worse” by adding some perturbations in the system.

The aim of chapter 3 is to explain these inclinations and eccentricities variations by having a look at the equations of motion.

3. The issue of high inclinations: explanations

3.1. Inclination vector evolution

The inclination and node evolutions of geostationary orbits have been extensively studied in the literature, we will just remind here some of the main results. As far as the node is concerned, the major difference between GEO and lower orbits is the impact of the third body perturbation. Kamel [8] illustrates the relative amplitude of the Earth’s oblateness (J_2) and luni-solar perturbation on the angles drift:

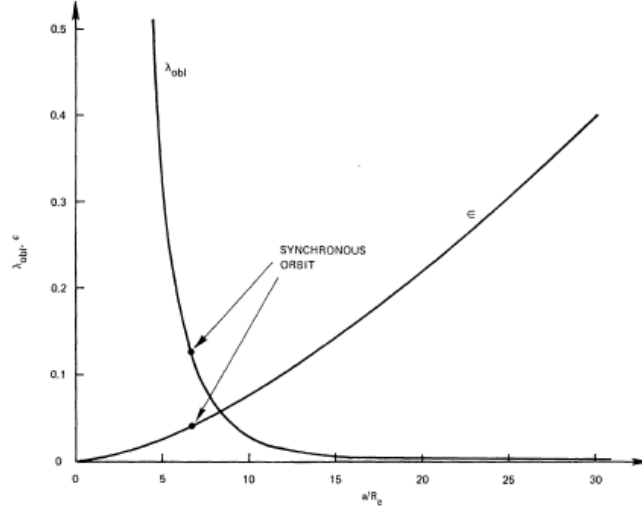


Figure 8: Oblateness (λ_{obl}) and luni-solar (ϵ) relative amplitude of perturbation vs. semi major axis

The main result from Fig.8 is that J2 and third body perturbations are of the same order of magnitude in GEO. Note that for Medium Earth Orbits (MEO), with a semi major axis about half the one in GEO, the luni-solar perturbation will be about 3 times lower whereas the J2 effect will be 11 times higher, making the Earth's oblateness the dominant perturbation.

Kamel solves the averaged equations of motion for small eccentricities and inclinations and demonstrates that the inclination vector, under the combined influence of Earth and third body perturbations, rotates around an equilibrium point given by RAAN $\sim 0^\circ$ and $i \sim 7.5^\circ$. As a consequence, it explains the classic evolution of a GEO disposal orbit whose inclination drift from 0° to about 15° periodically.

The equilibrium point defines an inertially fixed orbital plane sometimes referred to as the Laplace invariable plane. The equilibrium point is well visible in Fig. 4 and 7. Note that its position slightly depends on the date, through the lunar node regression, whereas Rosengren [9] gives the influence of SRP on the inclination of the Laplace plane for HAMR.

We also see in Fig. 4 and 7 some small variations of the inclination for initial inclinations between about 70° and 110° (represented by blue circles): let us have a look on the equations to explain it.

Ref. [10] gives the simply averaged (over the satellite orbit) keplerian equations of motion due to the third body perturbation. To study the inclination and RAAN derivatives it is convenient to use a frame oriented towards the ascending node rather than towards the perigee: using the same notations as in Ref. [10] and after a rotation of ω (Argument of Perigee) around the Z axis we get:

$$\begin{cases} \frac{di}{dt} = \frac{3}{2} \frac{\mu}{nd^3} \frac{Z}{\sqrt{1-e^2}} \left[[1 + e^2(5\cos^2\omega - 1)]X + \frac{5}{2}e^2\sin(2\omega)Y \right] \\ \frac{d\Omega}{dt} = \frac{3}{2} \frac{\mu}{nd^3} \frac{Z}{\sin(i)\sqrt{1-e^2}} \left[\frac{5}{2}e^2\sin(2\omega)X + [1 + e^2(5\sin^2\omega - 1)]Y \right] \end{cases} \quad (3)$$

With d the distance between the center of the Earth and third body, μ the gravitational constant of the third body and (X, Y, Z) the components of the third body position unit vector in the (N, Q, W) frame, where N is the direction of the ascending node and W to the orbit angular momentum. We can also express (X, Y, Z) as a function of the 3rd body keplerian elements (tagged with a b-index). Considering that the 3rd body orbit is circular we get:

$$\begin{pmatrix} X \\ Y \\ Z \end{pmatrix} = \begin{bmatrix} \cos(\Delta\Omega)\cos(M_b) + \sin(\Delta\Omega)\cos(i_b)\sin(M_b) \\ -\sin(\Delta\Omega)\cos(i)\cos(M_b) + [\cos(\Delta\Omega)\cos(i)\cos(i_b) + \sin(i)\sin(i_b)]\sin(M_b) \\ \sin(\Delta\Omega)\sin(i)\cos(M_b) + [-\cos(\Delta\Omega)\sin(i)\cos(i_b) + \cos(i)\sin(i_b)]\sin(M_b) \end{bmatrix} \quad (4)$$

With $\Delta\Omega$ being the difference between the orbit RAAN and the 3rd body RAAN.

By introducing Eq.4 in Eq.3 we are then able to compute the doubly averaged equations of motion by averaging over the third body mean anomaly M_b , assuming that the others parameters are constant:

$$\begin{cases} \frac{d\bar{i}}{dt} = \frac{1}{2\pi} \int_0^{2\pi} \frac{di}{dt} dM_b \\ \frac{d\bar{\Omega}}{dt} = \frac{1}{2\pi} \int_0^{2\pi} \frac{d\Omega}{dt} dM_b \end{cases} \quad (5)$$

We plot the inclination derivatives values coming from Eq.5 for the initial conditions of test case 1, for the Sun and Moon perturbation:

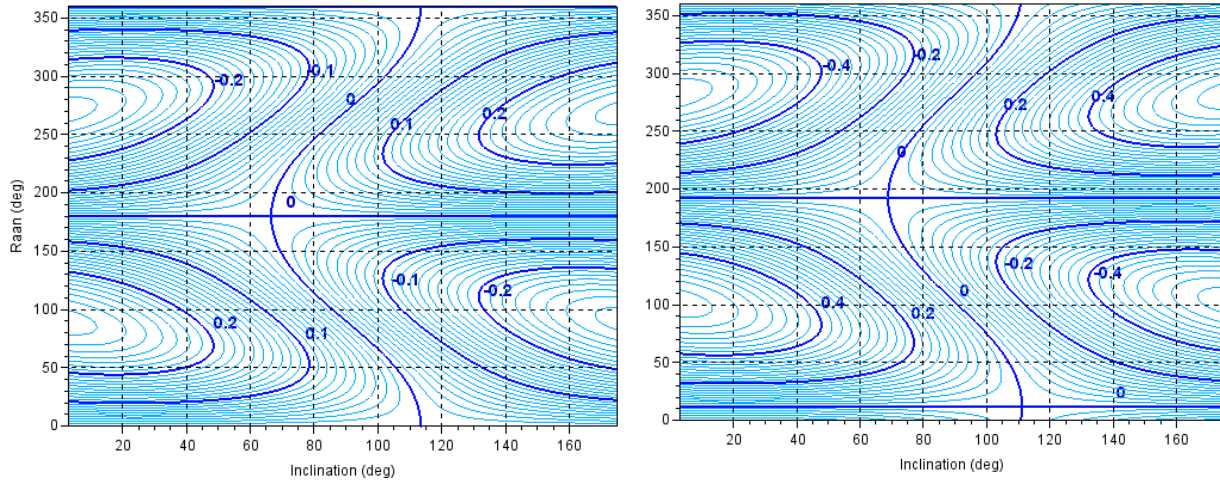


Figure 9: Inclination derivatives (deg/year) due to Sun (left) and Moon (right) as a function of inclination and RAAN

One can see from Fig.9 that the effect of Sun perturbation on the inclination is null for $RAAN=0^\circ$ or 180° as well as for particular values of RAAN for inclinations between 70° and 115° , which explain the low inclination variations (blue circles) in this range of inclinations in Fig.4 and 7. We have the same shapes for the Moon perturbation, shifted because of the non-zero value of the Moon RAAN, which is 12° at the initial date of test case 1. Fig. 9 is very consistent with

the propagation results in Fig.4 and 7, keeping in mind that these derivatives of Fig. 9 are just the initial values, with zero eccentricity.

We plot the RAAN derivatives from Eq.5, completed with the J2 drift contribution, for initial conditions of test case 1. It confirms the equilibrium point in {8, 0} and the slow inclination vector drift for inclinations near 90°.

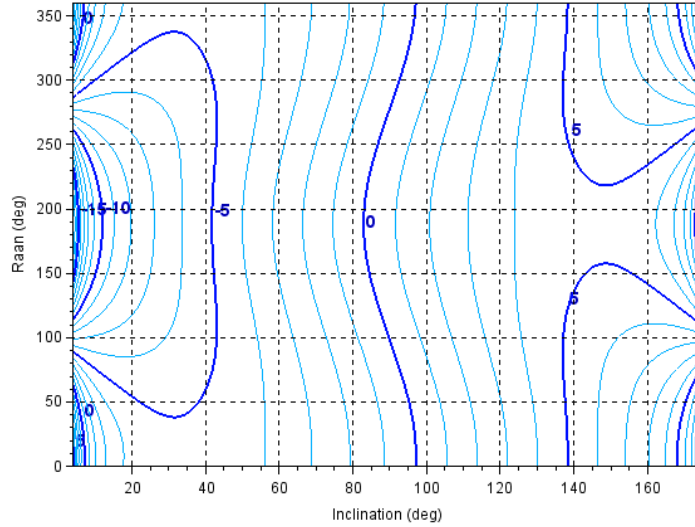


Figure 10: RAAN derivatives (deg/year) due to Sun, Moon and J2 as a function of inclination and RAAN

Due to the small values of the RAAN derivatives for some inclinations (quasi polar in particular), the RAAN will not always perform a complete rotation during 100 years of propagation. If we perform the propagation over a longer time span it will allow the geometry between the orbit and the third bodies to cover more possibilities and consequently more resonance conditions could be met.

3.2. Eccentricity evolutions

Due to the quite slow variations of the orbit angles and the long time span we are interested in, the eccentricity evolution is well described by the doubly averaged (over the satellite mean anomaly and the third body mean anomaly) equations of motion for third body perturbation [11]:

$$\left(\frac{d\bar{e}}{dt}\right)_{3rd\ body} = -\frac{15}{4} \frac{e\sqrt{1-e^2}}{n} \frac{\mu}{d^3} \sum A_k \sin(\Phi_k) \quad (6)$$

With A_k and Φ_k given by Tab.3, $\Delta\Omega$ being the difference between the orbit RAAN and the 3rd body RAAN.

Table 3 : Coefficients for doubly averaged eccentricity derivative

A_k	Φ_k
-------	----------

$3/4 (\sin^2(i_b) - 1/2) \sin^2(i)$	2ω
$1/4 \sin(2i_b) \sin(i) (1 + \cos(i))$	$2\omega + \Delta\Omega$
$-1/4 \sin(2i_b) \sin(i) (\cos(i) - 1)$	$-2\omega + \Delta\Omega$
$-1/8 \sin(i_b)^2 (1 + \cos(i))^2$	$2\omega + 2\Delta\Omega$
$1/8 \sin(i_b)^2 (\cos(i) - 1)^2$	$-2\omega + 2\Delta\Omega$

We can plot the amplitudes Ak for the Sun perturbation; it gives a first indication on why the eccentricity variations are higher for high inclinations:

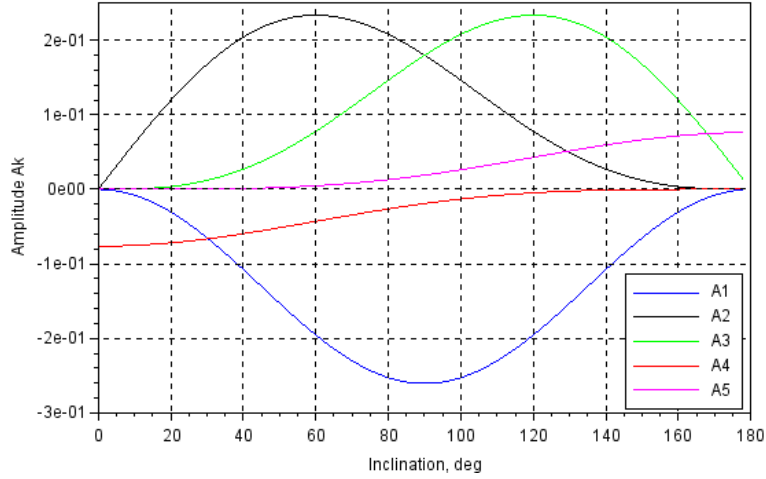


Figure 11: Amplitudes of coefficients vs. inclination – Doubly averaged equation

All the terms in Eq.6 are *a priori* periodic, even if the rotation periods of the angles Φ_k are significantly shorter in GEO than in LEO. We consider that a resonance is met when a term which was periodic becomes secular. In LEO the condition of resonance can be written as follows:

$$\exists k : \frac{d\Phi_k}{dt} \approx 0 \quad (7)$$

The classic study of resonances in LEO consist in solving Eq.7 : it can be done easily since the angles derivatives are dominated by the J2 drift and are consequently a function of the semi-major axis, eccentricity and inclination only [11]:

$$\left. \frac{d\Phi_k}{dt} \right)_{LEO} = f(a, e, i) \quad (8)$$

However, we have seen in Fig.8 that in GSO the luni-solar perturbation is of the same order of magnitude than the Earth's oblateness effect. Therefore, the angle derivatives are not only a function of (a, e, i) but also of the angles themselves. Eq.8 becomes:

$$\left. \frac{d\Phi_k}{dt} \right)_{GSO} = g(a, e, i, \omega, \Omega) \quad (9)$$

As an example, Fig.10 is the plot of the RAAN derivatives with fixed values of three parameters: $g(42464 \text{ km}, 0, i, 0, \Omega)$. These dependencies make the study of the resonances even more complex since the condition from Eq.7 is necessary but not sufficient to get a resonance since the derivative may vary if the Argument of Perigee or the RAAN drift. A more accurate definition of a resonance condition for GSO is when the 3 following conditions are met:

$$\exists k : \begin{cases} \frac{d\Phi_k}{dt}(a, e, i, \omega, \Omega) \approx 0 \\ \left\{ \frac{d\omega}{dt} \approx 0 \right\} \cup \left\{ \frac{\partial}{\partial \omega} \left(\frac{d\Phi_k}{dt} \right) \approx 0 \right\} \\ \left\{ \frac{d\Omega}{dt} \approx 0 \right\} \cup \left\{ \frac{\partial}{\partial \Omega} \left(\frac{d\Phi_k}{dt} \right) \approx 0 \right\} \end{cases} \quad (10)$$

A complete study of those three conditions is tedious since we have to deal with 5 variables (6 if we take into account the drift of the Moon RAAN). However, we can get meaningful information by studying only the first condition since it is a necessary condition for the resonance to happen. Fig.12 gives, for each one of the five angles from Tab.3, the minimum absolute value of the derivatives as a function of the inclination and eccentricity, whatever the AoP and RAAN:

$$\min_{\substack{\omega \in [0, 2\pi] \\ \Omega \in [0, 2\pi]}} \left| \frac{d\Phi_k}{dt}(a = 42464 \text{ km}, e, i, \omega, \Omega) \right| \quad (11)$$

J2 and the luni-solar perturbations are taken into account. We are interested in the dark blue areas in Fig.12 since they indicate that it exists a couple (AoP / RAAN) so that for these semi-major-axis, eccentricity and inclination get very slow variations of the Φ angles. As stated before, it is not a sufficient condition to get a resonance since the AoP or the RAAN may drift and increase the Φ variations. However, it is a necessary condition, which implies that resonance are likely to happen only for the inclinations ranges associated with dark blue areas: the union of these ranges for the 5 angles from the doubly averaged equations for eccentricity (Eq.6) is about $[30^\circ, 150^\circ]$. This is very consistent with the results coming from our test cases: we can see in Fig. 5 that the high eccentricities are contained within this range of inclinations.

From the left plot of Fig.5 we can wonder why the maximum eccentricity seems lower around 80° of inclination: it is a consequence of the very slow rotation rate we can get on the angles AoP, RAAN or Φ : a few degrees a year. As a consequence, propagating over a 100 years' time span may not be enough to reach the maximum eccentricity allowed by the initial conditions: as an example we propagated again some of the initial conditions for the inclination range $[50^\circ, 130^\circ]$ (which is a reduced inclination range to save computation time) over a 1000 years' time span and we plot the eccentricity evolution as a function of the inclination for hundreds of propagation in Fig. 13.

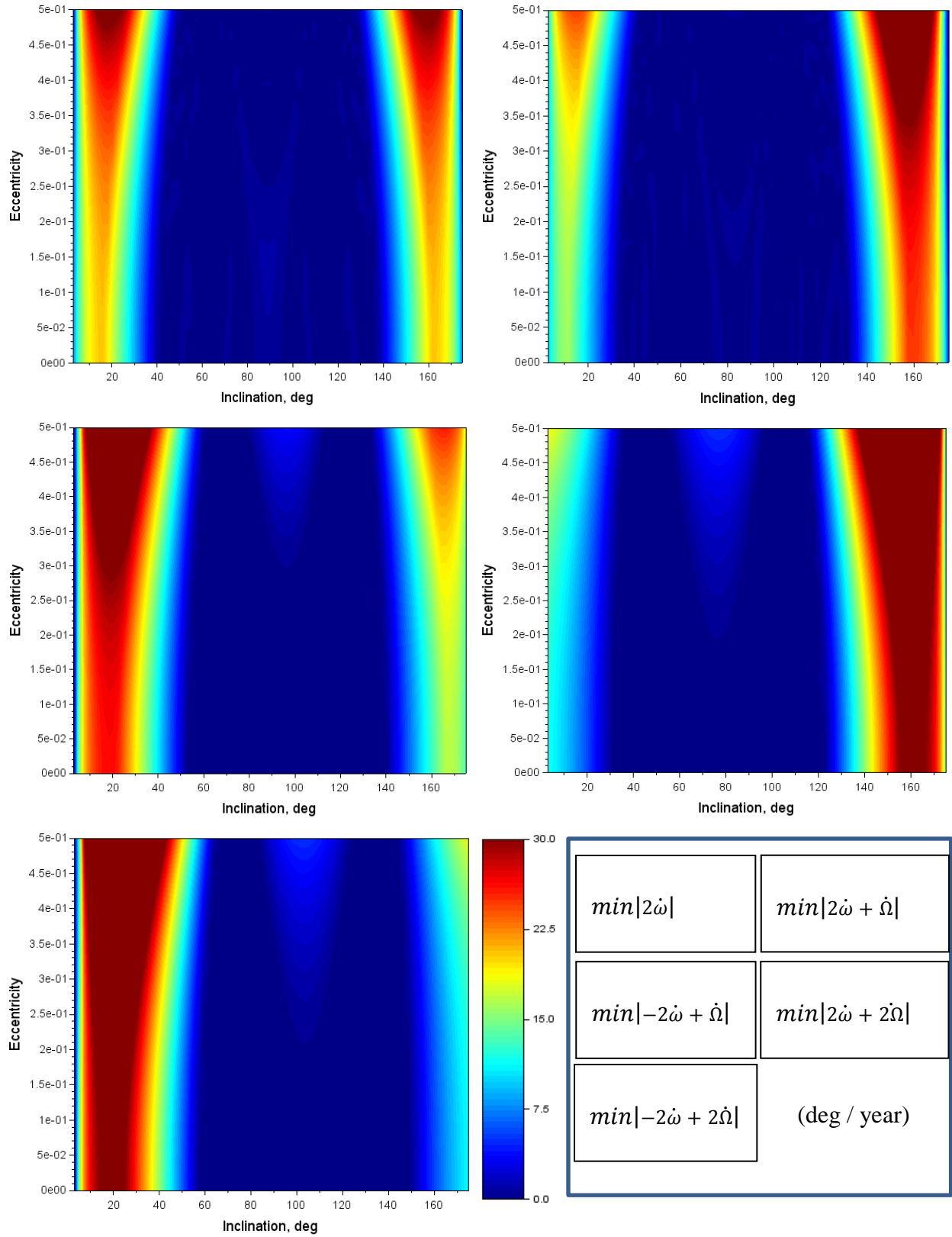


Figure 12: Φ_k Angles derivatives (deg/year) vs. Inclination and Eccentricity

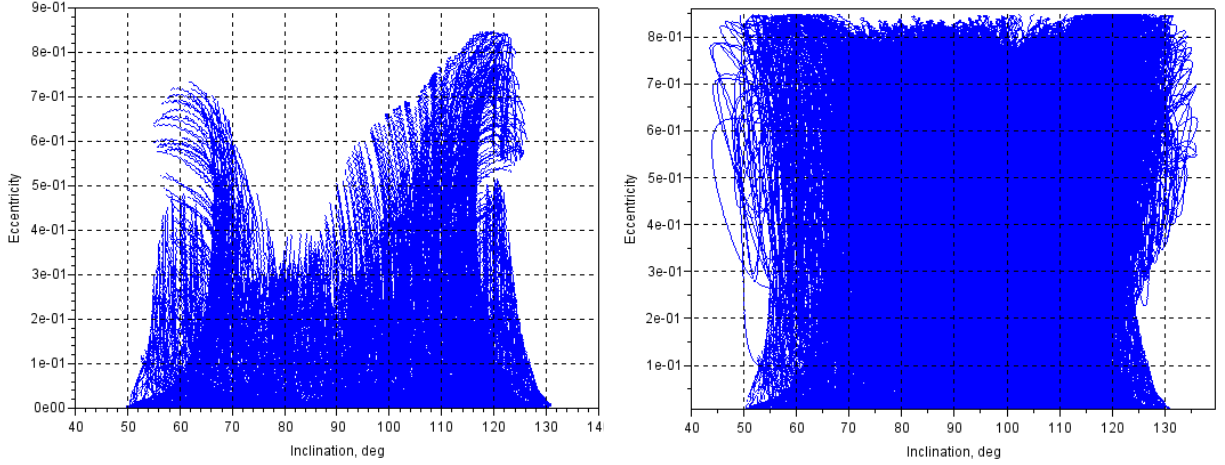


Figure 13: Eccentricity vs. inclination over 100 years (left) or 1000 years (right)

One can see from Fig.13 that in this inclination range, propagating over 100 years is not enough to get the full picture of the eccentricity evolution. Note that none of those initial conditions was “stable”: we notice a huge increase in the eccentricity in all cases after a long enough time span (which is consistent with the MEGNO values from Fig.6). If we propagate long enough, the natural evolutions of RAAN, AoP and inclination make that some resonances on the eccentricity always occur.

Now that the eccentricity variations due to third body have been detailed, we give the singly averaged equations of the Solar Radiation Pressure impact on the eccentricity:

$$\left(\frac{d\bar{e}}{dt}\right)_{SRP} = -\frac{3\sqrt{1-e^2}}{4} \frac{K}{na} \sum B_k \sin(\Psi_k) \quad (12)$$

One should refer to [11] for more details, but all the Ψ angles depend on the Sun right ascension, therefore we cannot get doubly averaged equations for SRP. Plus, due to the low rotation rate of AoP and RAAN, the Ψ angles will have a rotation rate near to the one of the Sun right ascension, that is to say a round per year: no resonances here. We can conclude that, keeping apart the HAMR objects which are out of the scope of this paper, the SRP will not be the dominant perturbation for GSO at high inclinations.

4. Disposal of geosynchronous satellites

4.1. Crossing of the GEO protected region

The orbit radius r and the geodesic latitude φ can be expressed as a function of the orbital elements, with v being the true anomaly:

$$\begin{aligned} r &= a \frac{1 - e^2}{1 + e \cos(v)} \\ \varphi &= a \sin(\sin(i) \sin(\omega + v)) \end{aligned} \quad (13)$$

To evaluate the crossing of the GEO protected region we consider a simple algorithm: for each point of the ephemeris, which is a mean point since we use a semi-analytical model, we spread 150 evaluation points equally (spread in mean anomaly) over the orbit. We compute the altitude and latitude for each of them using Eq.13. No short periodic terms are added, which means we neglect the short periodic variations. There is a crossing of the protected region if the latitude is within $[-15^\circ; 15^\circ]$ AND if the altitude is within $[\text{GEO} - 200\text{km}; \text{GEO} + 200\text{km}]$. Note that by counting the evaluation points that lie within the protected region we get a percentage of crossing over 100 years. It is important to consider both conditions given above: since we are interested in GSO at “high” inclinations, it is possible to have points with latitude higher than 15° whereas their altitude is within the protected range. Figure 14 gives an example of such a compliant orbit over 100 years, with initial inclination around 60° :

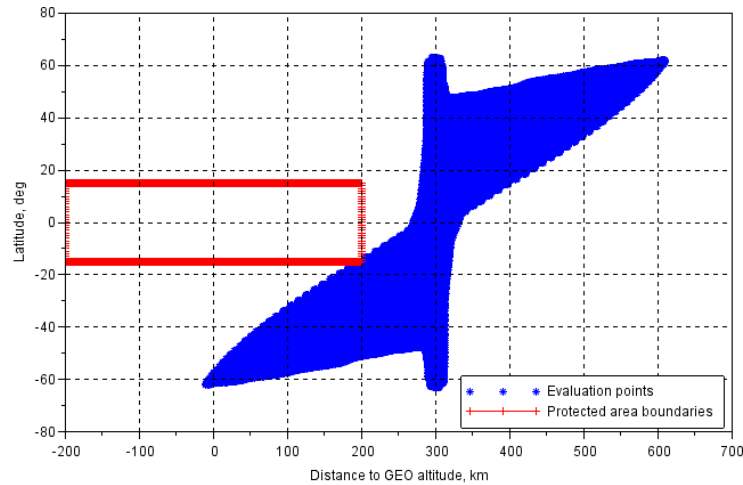


Figure 14: Latitudes and Altitudes for a compliant orbit over 100 years

We can plot, for example for a semi major axis of 42464 km (GEO+300km) the distance to the GEO altitude as a function of the orbit eccentricity and the true anomaly:

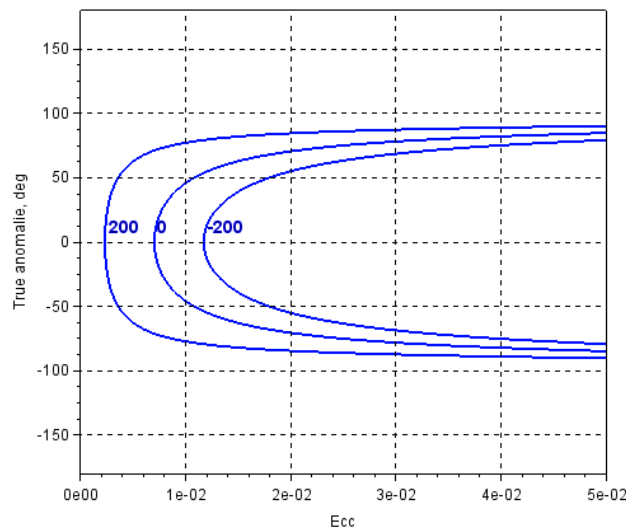


Figure 15 : Distance to the GEO altitude (km) vs. eccentricity and true anomaly

For a given eccentricity, the blue lines indicate the anomaly of entry and exit within the protected altitude range; it is an indication of the time potentially spent in the GEO protected area, even if a plot in mean anomaly would be better suited to visualize it. We can deduce from Fig. 15 that having a large eccentricity can reduce the amount of time spent in the protected region.

We also plot the latitude as a function of the orbit inclination and the argument of latitude ($\omega+v$):

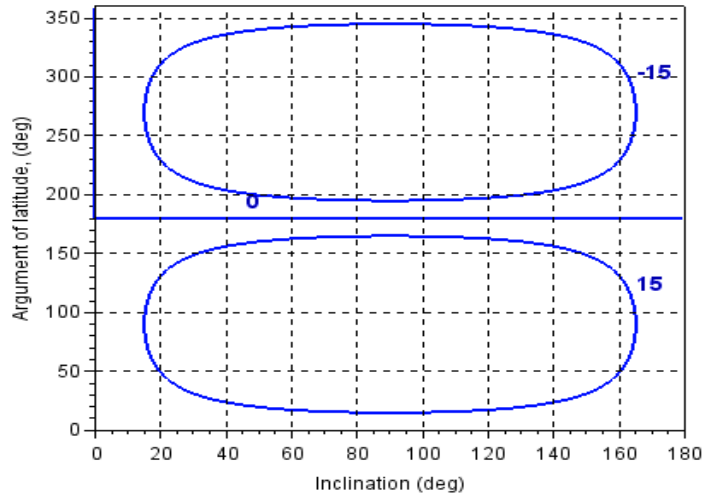


Figure 16 : Latitude (deg) as a function of inclination and Argument of latitude

The points within the two blue ellipses in Fig. 16 have latitudes outside the latitude protected range $[-15^\circ, 15^\circ]$. Figure 16 illustrates the fact that, depending on the orbit inclination, an orbit with a “high eccentricity” can be compliant if the AoP is placed so that the argument of latitude corresponding to the true anomaly values from Fig. 15 are contained within the blue ellipses. Note that the very same algorithm presented above can be used to detect the crossing of the GEO control box (station keeping box for operational GEO satellites, defined here by ± 40 km around GEO altitude and $\pm 5^\circ$ of latitude).

It is important to keep in mind that the crossing of the protected region is a function of the semi-major-axis, inclination, eccentricity and argument of perigee. Since we are unable to predict *a priori* their evolution over long time span, we are unable to predict how or when the crossing will happen: we have to propagate the orbit to evaluate it.

4.2. Towards a disposal strategy for GSO

From the previous chapters we conclude that strong variations on the eccentricity are inevitable for GSO with an initial inclination within the range $[30^\circ; 150^\circ]$. As a consequence, it is obvious that the ISO formula (Eq. 1) cannot be used anymore in these cases to select an appropriate disposal orbit. From now on, we postulate that any disposal orbit within the critical range of inclinations will cross the GEO protected area, even if it is after a very long period of time (centuries...). As a consequence, since we cannot avoid crossing the protected region, we need another criterion to determine what disposal strategy is the best. Two examples of criteria are proposed here (but better ones could maybe be found):

- GSO_C1: “The rate of crossing of the GEO protected region should be lower than 0.xx “. The rate of crossing being defined by the amount of time spent in the protected region

divided by the time of propagation. For GSO within the critical inclination range the rate of crossing will not be zero over a very long time span since the crossing will happen.

- GSO_C2: “The disposal orbit should not cross the GEO protected region within the first XXX years after the date of disposal”. This criterion already exists for GEO and is used with a 100 years value. To be consistent, we propose to use this value also for GSO, keeping in mind the fundamental difference: a compliant GEO satellite will never cross the protected region (due to the “weak dynamics” for such orbits), whereas a GSO satellite compliant with GSO_C2 will cross the protected region (but after 100 years).

Both criteria follow the global idea that the disposal orbit “quality” should be evaluated through the collision risk with operational GEO satellites (which is hard to evaluate directly), by cancelling the risk during the first 100 years (GSO_C2) or by minimizing it over the years (GSO_C1). Note that we are going to see in the next chapters that this simple definition has to be completed by a statistical approach.

Before evaluating these criteria on a concrete example, let us first consider what are the available “degrees of freedom” in our selection of the disposal orbit:

Table 4 : Degree of freedom for the disposal orbit

Parameter	Degree of freedom?	Comments
Semi major axis	Yes	Weak impact on the dynamic.
Inclination	No	Cost of out of plane manoeuver is too high.
RAAN	Rather no	Cost of out of plane manoeuver is too high. Linked to the date since it is drifting, but slowly.
Eccentricity vector (e,ω)	Yes	Existence of an optimal eccentricity vector?
Date	Rather no	We can wait for an “optimal date” (if it exists) but we also need a disposal strategy whatever the date is since the end of mission date is not precisely known.
Spacecraft characteristic	Yes	Weak impact on the dynamics since SRP is not the dominant perturbation.

In Tab. 4 we considered that the initial inclination vector (see Eq.2), whose importance have been proven in the previous chapters, will probably not be a degree of freedom since the manoeuver cost to change it would be too high and its natural drift would be too slow (a few degrees per year for RAAN). The semi-major axis will be raised above GEO in most of the case but its variation will not have a strong impact on the orbit evolution. The main parameter we can select is the eccentricity vector: for GEO satellites at low inclinations, tables indicate the optimal eccentricity vector as a function of the date of disposal [3]. The basic idea is to have a perigee correctly oriented w.r.t the Sun since the SRP is the dominant perturbation in these cases. It is not true anymore for GSO within the critical inclination range, but we can wonder whether we can find or not an “optimal eccentricity vector” (optimal w.r.t one of the criteria). Due to the high number of variables (orbit, spacecraft characteristics...) and the complexity of the analysis of the resonances, we will not study this problem in the general case but focus on a particular example. Parameters of test case 3 are given in Tab.5:

Table 5 : Test case 3 parameters

Initial date	2020-01-01
Semi major axis	GEO + 300 km
Eccentricity vector (e, ω)	Degree of freedom
Inclination	55° (operational GSO satellites have been found at this inclination)
Right Ascension of Ascending Node	0° (arbitrary)
Area to mass ratio	0.01 m ² /kg (classic value)
Force model	Earth potential (7x7 model), Sun potential, Moon potential. Solar Radiation Pressure
Propagation time	100 years
Propagation method	Semi-analytical (STELA)

4.3. Minimizing the rate of crossing of the GEO protected region

Figure 17 gives the percentage of time spent in the GEO protected area for test case 1:

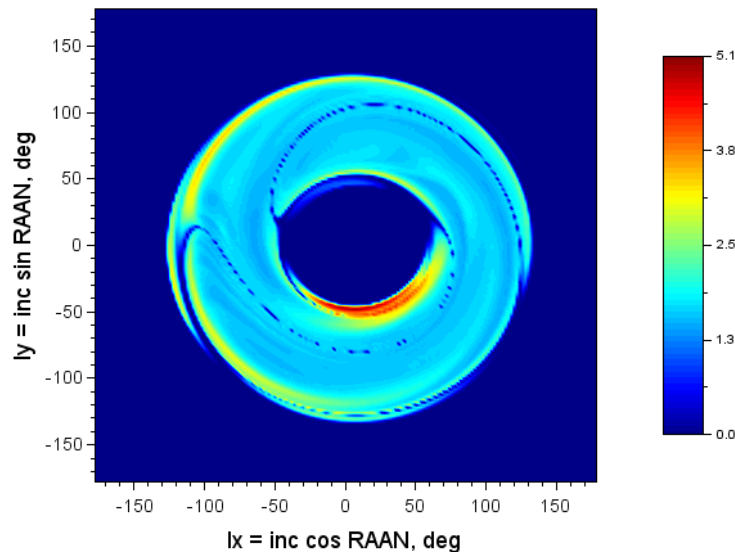


Figure 17: Percentage of time spent in the GEO protected area vs. initial inclination vector

Our calculations show that 45% of the initial conditions from test case 1 lead to a crossing of the GEO protected area (points in Fig 17. that are not in dark blue color). Also, 39% of the initial conditions lead to a crossing of the GEO control box! We notice from Fig.17 that the maximum value we get is about 5% of the time spent in the GEO protected area (0.5% if we are interested in the GEO control box). Also, no particular relation is visible between the rate of crossing and the maximum eccentricity, which was expected since we demonstrated that the crossing of the protected region is a function of 4 orbital parameters. The blue lines in the critical inclinations range indicate compliant orbits, such as the one plotted in Fig. 14. It is important to keep in mind that it comes from the fact that we propagated over 100 years “only”. If we propagate over a

longer time span all these blue lines will vanish when the eccentricity increases and/or the AoP drifts, even very slowly.

We now study the results from test case 3: here, the initial eccentricity is chosen between 0 and 0.025 (26 different values), with an Argument of Perigee between 0° and 360° (10° step) which represents about 900 propagations. Figure 18 gives the percentage of time spent in the GEO protected area over 100 years:

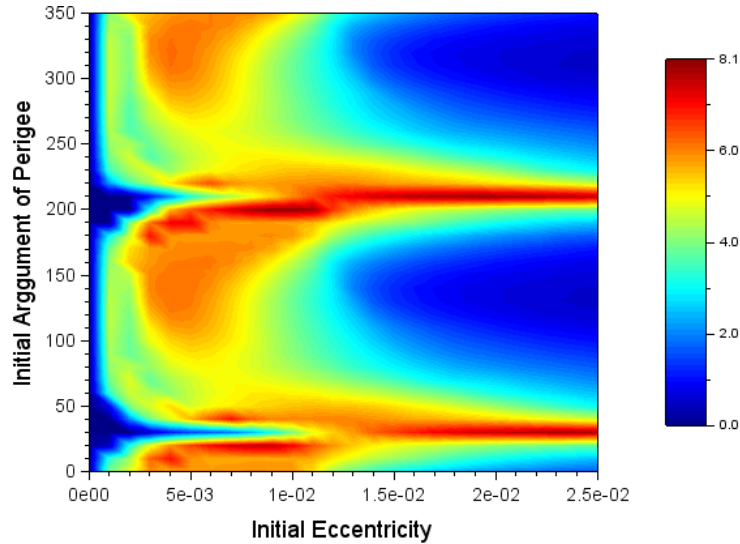


Figure 18: Percentage of time spent in the GEO protected area over 100 years vs. initial eccentricity vector – Test case 3

For an initially circular orbit ($e=0$) there is no GEO crossing over 100 years. We see in Fig. 18 two particular values of the Argument of Perigee: 30° and 210° . Of course these values depend on the initial conditions (mostly the inclination vector) and will not be the same for another test case. It is quite logical that those values are separated from 180° since all the Φ angles in Tab.3 are a function of two times the AoP so we can expect a pi-periodicity. The small differences in the signatures for these two values are probably coming from the Solar Radiation Pressure.

Figure 19 shows the eccentricity evolutions for the propagations with an initial AoP of 30° , which is in this case the most “optimal” one, and an initial eccentricity lower or equal to 0.01:

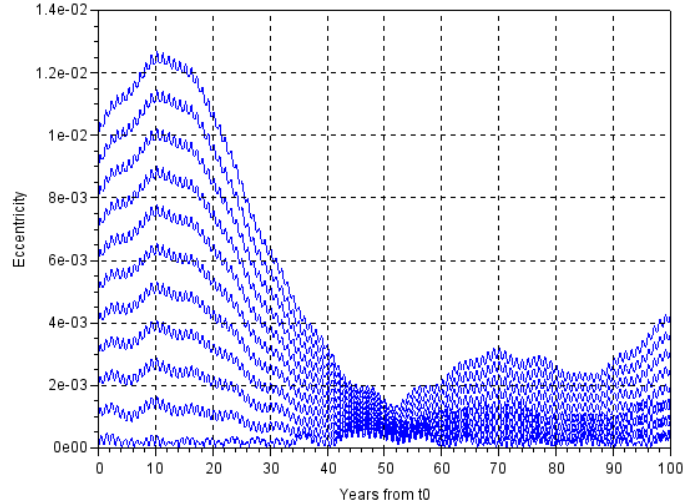


Figure 19: Eccentricity evolutions for "stable" AoP

We can see in Fig.19 the small eccentricity oscillations of negligible amplitude due to SRP, with a period of about one year. To study the impact of the third body perturbation we plot the eccentricity derivatives computed from Eq. 6 for the propagation case with an initial eccentricity of 0.01, as well as the term by term decomposition from Tab.3:

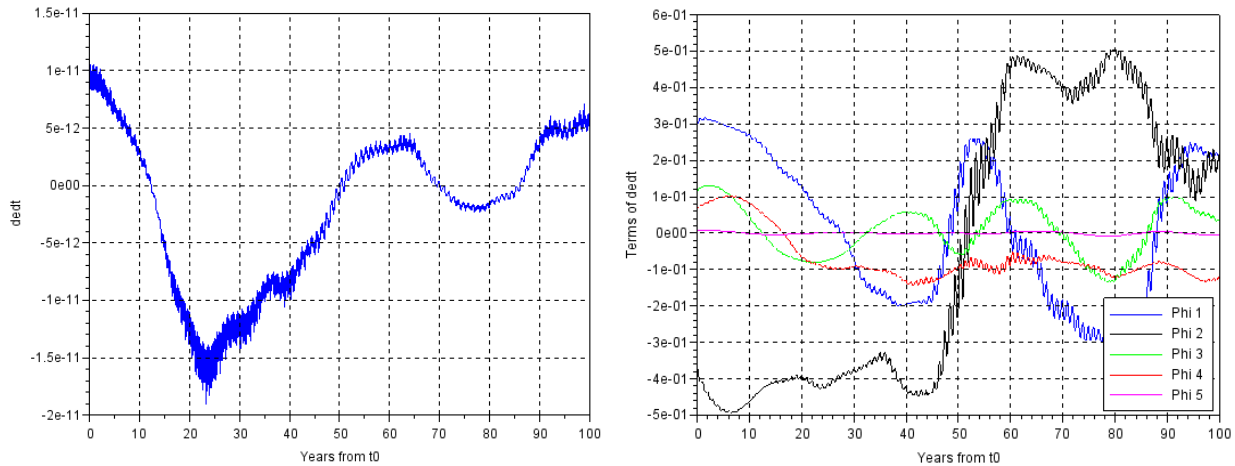


Figure 20: Eccentricity derivatives (day^{-1}) due to third body (sum and term by term)

The eccentricity derivatives due to third body are very consistent with the eccentricity evolutions in Fig 19. The derivative is positive during the first 10 years, leading to a global increase of the eccentricity, then negative between 10 and 50 years of propagation, etc. The term by term decomposition shows that all the angles are slowly drifting but the main ones are 2ω and $2\omega+\Delta\Omega$. It is worth noting that for the “optimal” value of the AoP (30°) the third body perturbation starts by increasing the eccentricity over the first years of propagation! It shows how hard (even impossible?) it is to identify the optimal initial conditions just by analyzing the effects of the perturbations at the date of disposal (i.e. without propagation).

We have seen that for a given initial condition the maximum eccentricity could be reached well after 100 years of propagation (see Fig.13). As a consequence, evaluating GSO_C1 over 100 years only is not particularly justified and worse, irrelevant: the “optimal” disposal orbit over

100 years might not be the same as the “true” optimal orbit we are interested in. As an illustration we plot the results from test case 3, but after 1000 years of propagation:

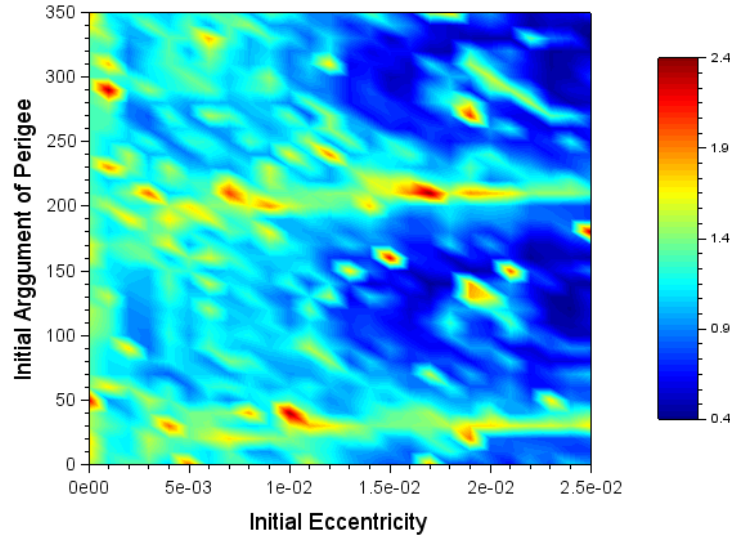


Figure 21: Percentage of time spent in the GEO protected area over 1000 years vs. initial eccentricity vector

We can see that the results are completely different after 1000 years of propagation from the ones of Fig.18. Also, we have no justification that the results have converged at this time: propagations after a longer time span could change the results again. As expected, all the initial conditions lead to a crossing of the GEO protected region, we also see that the low eccentricity values do not seem optimal anymore. The irregularities of the plot are an illustration of a phenomenon we haven’t talk about yet: because of the strong orbital resonances, the results can be very sensitive to initial conditions, particularly after a very long propagation time. Figure 22 gives the eccentricity evolution over 1000 years for an initially circular orbit with 15 randomly chosen dates within the 1st and the 7th of January, and a randomly chosen value of the reflectivity coefficient (+/-20% uniform dispersion over the nominal value):

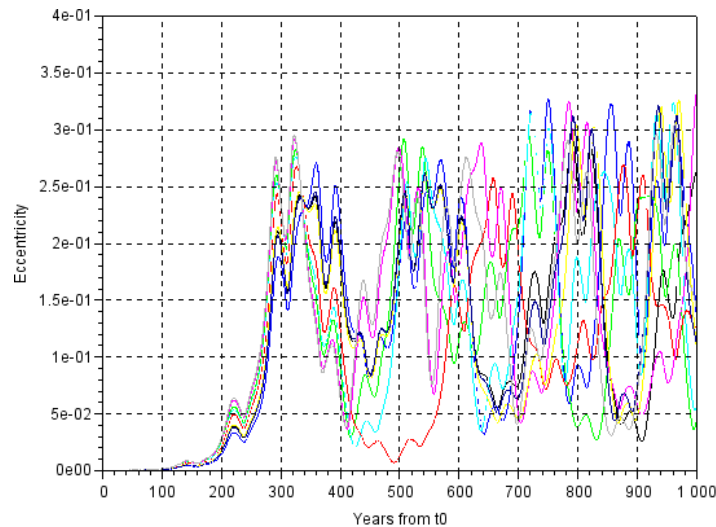


Figure 22: Eccentricity evolution over 1000 years, small changes in the initial conditions

We can see that the eccentricity exhibits a chaotic behavior, with a huge impact of small differences in the initial conditions on the orbit evolution and, consequently, on the criteria: the rate of crossing of the GEO protected region changes in this case of a ratio from 1 to 5 between the propagations. As a consequence, the criteria GSO_C1 should not be checked using a single extrapolation: a statistical approach is required. The same consideration were faced when establishing the criteria to check the compliance of GTO disposal orbits with respect to the technical regulations attached with the French Space Operations Act [12]. Following the same strategy, we can define statistical criteria for the GSO:

- **GSO_SC1:** “The rate of crossing of the GEO protected region should be lower than 0.xx with a 0.yy probability level “.
- **GSO_SC2:** “The disposal orbit should not cross the GEO protected region within the first 100 years after the date of disposal, with a 0.yy probability level”.

GSO_SC1 is an interesting criterion since the rate of crossing of the GEO protected region is somehow related to the total risk of collision. However, using this criterion to try to find the “best” disposal orbit (in particular the optimal eccentricity vector) appears to be difficult in practice:

- We don’t know what propagation duration is necessary for the rate of crossing to reach its converged value.
- We cannot identify *a priori* (i.e. without propagation) the optimal eccentricity vector due to the complexity of the orbit evolution.
- A scan of the initial possible eccentricity vectors with a single propagation is not useful to identify the optimum since results from one single propagation are not stable.
- A scan of the initial possible eccentricity vectors using statistical analysis (Monte Carlo simulation) to identify the optimum would be too much expensive from a computation time point of view.

4.4. Delaying the first crossing of the GEO protected region

The initial eccentricity for test case 3 is chosen between 0 and 0.01 (26 different values), with an Argument of Perigee between 0° and 360° (10° step) which represents about 900 propagations. Figure 23 gives the date of first crossing of the GEO protected area (values equal to 100 years mean that no crossing was detected during the 100 years of propagation).

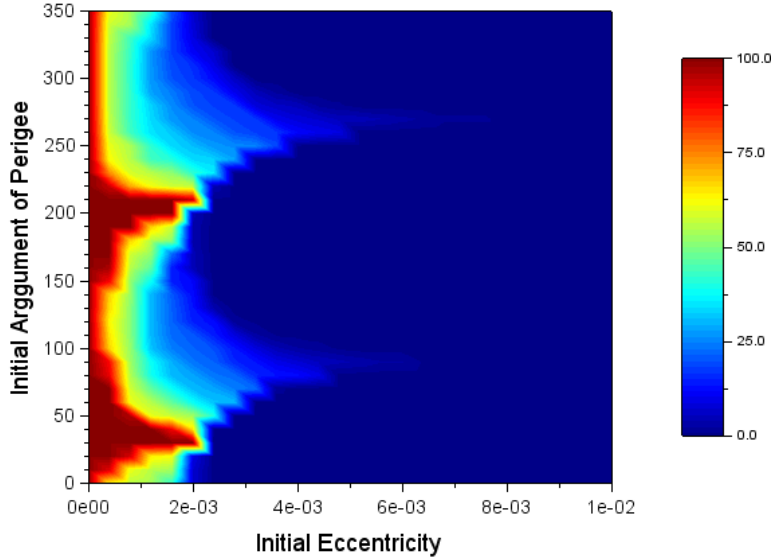


Figure 23: Duration (years) before first crossing of the GEO protected region (100 years propagation) – Test case 3

We see once again two particular values of the AoP (30° and 210°), separated from 180° , that seem optimal with respect to the GSO_C2 criterion. Of course, targeting a circular orbit is a good way to minimize the eccentricity variation and consequently to delay the date of first crossing; we can see that directly from Eq. 6. However, one should keep in mind that a zero eccentricity is not achievable operationally (incertitude on the remaining propellant, efficiency of the last burst, etc.). Therefore, targeting a non-zero eccentricity but with the optimal AoP is a better option here. Due to the choice of the semi-major axis (GEO +300 km) the disposal orbit can cross the GEO protected region for eccentricity higher or equal than $2.3e-4$: it explains the dark blue area with a crossing within the first year on the right side of Fig. 23. Of course we will have a higher value for this “limit eccentricity” if the semi-major axis of the disposal orbit is higher.

The results here are not sensitive to the propagation duration, but we still need to perform a statistical analysis to evaluate how sensitive they are to a dispersion of the input parameters. As for GSO_C1, the ideal strategy would be to identify the “true” optimal eccentricity vector by scanning the initial eccentricity vectors and performing a statistical propagation for each of them, but it would be too much expensive from a computation time point of view. However, the initial conditions we are interested in here are those for which the eccentricity remains low for decades, in other words those that do not lead to a strong resonance on the eccentricity during the first decades. As a consequence, we can assume that an initial eccentricity vector selected from a favorable area after a single extrapolation (such as the dark red areas in Fig.23) should not be far away from the true (and also stable) optimal eccentricity vector.

As an example we select $(e,\omega) = (1.2e-3, 30^\circ)$ as the targeted eccentricity vector. We then perform a Monte Carlo simulation using the STELA software. STELA can perform a Monte Carlo simulation with a user-defined scattering of the input parameters, and evaluate the statistical criteria that have been defined to check the compliance of disposal GTO orbits [12], one of them being equivalent to our GSO_SC2. The scattering of the input parameters has been arbitrarily chosen and is given in Tab.6. The incertitude on semi major axis corresponds to an uncertainty on the last manoeuver of about 0.5 m/s, no correlations are considered between the orbital parameters uncertainty.

Table 6 : Dispersions for the Monte Carlo simulation

Initial date	Uniform dispersion between 2020-01-01 and 2020-04-01	
Semi major axis	+/- 15 km	Uniform dispersion
Eccentricity vector (e, ω)	+/- $3e-4$ and +/- 15°	Uniform dispersion
Inclination	+/- 1°	Uniform dispersion
Right Ascension of Ascending Node	+/- 1°	Uniform dispersion
Area to mass ratio times reflectivity coefficient	+/- 20%	Uniform dispersion

STELA gives the observed probability to stay outside the GEO protected region within 100 years, bounded by a Wilson 95% confidence interval [12]. For the propagation cases that do cross the protected region, the first date of crossing is sadly not saved by STELA. Figure 24 gives the results for 115 random propagations:

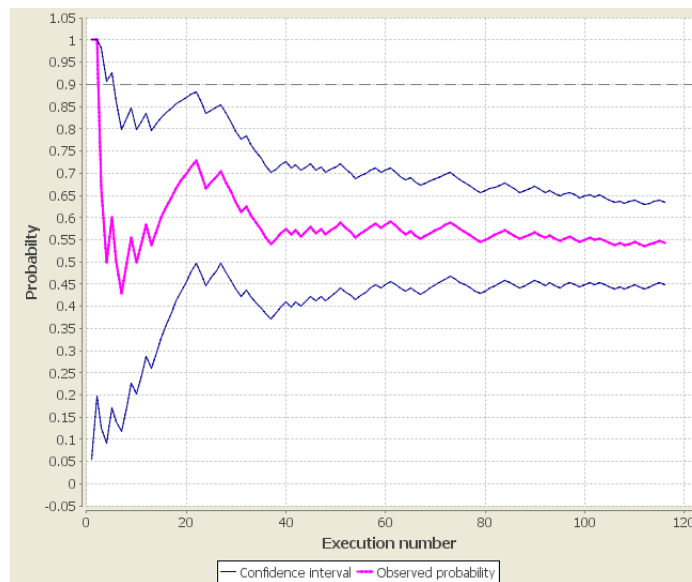
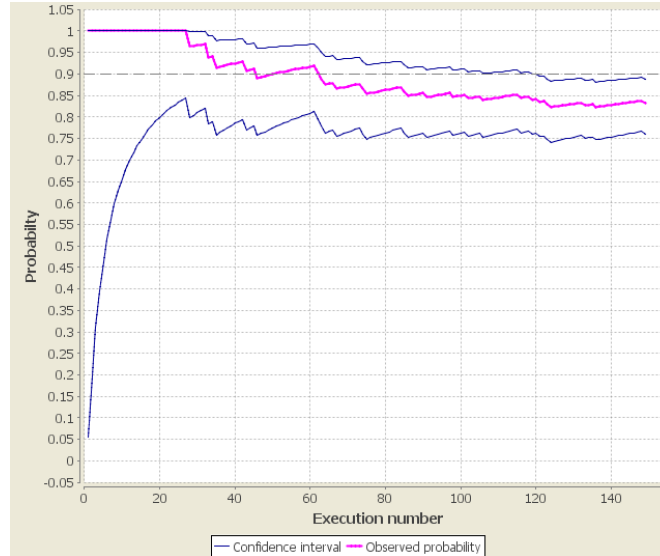


Figure 24: Probability of non-crossing of the GEO protected region within 100 years - sma ~ GEO+300 km

We see that for this disposal orbit and considering these initial dispersions on the input parameters, the probability to be compliant with GSO_C2 is about 0.55. If we consider that this probability is not high enough (depending on the probability adopted in GSO_SC2) we just need to raise the semi-major-axis a little bit more, assuming that the optimal eccentricity vector is not sensitive to a small change in the semi-major axis of the disposal orbit. We perform the very same statistical analysis but with a semi-major-axis 100 km higher than before (GEO +400 km): we get a probability of 0.85, which is much better (see Fig. 25). By increasing again the semi major axis we could get a probability higher than 0.9, which is the probability used in the definition of the statistical criteria for GTO [12]. Note that it is *a priori* possible that for some inclination vectors we are unable to find a high enough probability to comply with GSO_C2: as a

consequence, the mission should be adapted so that this particular inclination vector is not reached at the end of mission.



**Figure 25: Probability of non-crossing of the GEO region within 100 years –
sma ~ GEO +400 km**

It appears that the criterion GSO_SC2:

- Is similar, thus consistent, with the criteria used in GEO and GTO for the crossing of the GEO protected region.
- Can be used in practice to discriminate what disposal orbit is better : we can identify an “optimal” eccentricity vector that delays the first crossing of the protected region:
 - A scan of the initial possible eccentricity vectors with a single propagation is useful to identify the stable areas.
 - A statistical propagation from a targeted eccentricity vector chosen within the stable area gives the probability of compliance we can expect taking into account the incertitude on the input parameters.
 - We can adjust the nominal semi-major-axis of the disposal orbit to get a high enough probability to be compliant with GSO_SC2 (if not, it means that we should change the mission orbit to have a different inclination vector at the date of disposal).
- However, one should keep in mind that:
 - The disposal orbit will cross the GEO protected region, even after centuries
 - Delaying the first crossing of the GEO protected region might not be the best way to minimize the total risk of collision over centuries.

6. Conclusions

The choice of the disposal orbit is relatively easy for typical geostationary satellites due to the smooth and predictable perturbations that affect these orbits. However, the disposal of space objects in geosynchronous orbits, which means at the geostationary altitude but with non-zero inclinations, can be more tedious, especially in the case of high inclinations. A critical inclination domain of $[30^\circ; 150^\circ]$ has been determined by analyzing the doubly averaged (mean anomaly and third body anomaly) equations for the eccentricity derivatives due to the third body

perturbation. This critical domain has been confirmed by the semi-analytical propagation of numerous test cases. Orbits within this inclination range will experience strong inclination and eccentricity variations: no stable points were found over centuries. The analysis of the resonances that leads to the eccentricity variations is tedious since the third body perturbation effect on the orbital angles (Right Ascension of Ascending Node and Argument of Perigee) are of the same order of magnitude as the Earth's oblateness and cannot be neglected.

As a consequence, we estimate that a spacecraft placed on a disposal orbit within this critical domain will cross the GEO protected region (and the GEO control box as well) whatever the initial conditions, even though it is after a 100-years-long period of time. From now on, in-flight missions within this critical inclination range are rare, which seems a good thing in the perspective of the protection of the GEO region.

Two criteria to evaluate the disposal orbits have been proposed. They are statistical criteria since the results coming from a single propagation might be very sensitive to the initial conditions, due to the chaotic behavior of the eccentricity evolution:

- GSO_SC1: "The rate of crossing of the GEO protected region should be lower than 0.xx with a 0.yy probability level".
- GSO_SC2: "The disposal orbit should not cross the GEO protected region within the first 100 years after the date of disposal, with a 0.yy probability level".

The pros and cons of each of these criteria have been analyzed from a particular example.

GSO_SC1 is an interesting criterion since the rate of crossing of the GEO protected region is somehow related to the total risk of collision. However, its practical use to find an appropriate disposal orbit appears to be delicate. GSO_SC2 is very consistent with existing criteria for GEO or GTO and its use appears to be easier to identify appropriate disposal orbits. However, one should keep in mind that delaying the first crossing of the GEO protected region might not be the best way to minimize the total risk of collision over centuries.

The choice of the probability level associated with these statistical criteria, seen as a compromise between the protection of the GEO region and the induced cost on the space system, as well as the "good practices" to normalize their computation (how to scatter the input parameters, how to handle the statistical variability...) are yet to be studied.

7. References

[1] http://www.ucsusa.org/nuclear_weapons_and_global_security/solutions/space-weapons/ucs-satellite-database.html

[2] Krag, H. "Review of Global Achievements in clearing LEO and GEO protected area" 31st IADC meeting, Darmstadt.

[3] ISO document 28672: Space systems – Disposal of satellite operating at geosynchronous altitude

[4] Le Fèvre, C. et al "Compliance of disposal orbits with the French Space Act: the good practices and the STELA tool". IAC 2012, Naples.

[5] Fraysse, H. et al "STELA, a tool for long term orbit propagation". ICATT 2012.

- [6] Cincotta. "Phase space structure of multi-dimensional systems by means of the mean exponential growth factor of nearby orbits". 2002.
- [7] Morand, V. "Semi Analytical computation of partial derivatives and transition matrix using STELA software". 6th ESA conference on space debris, 2013.
- [8] Kamel, A. "Some useful results on initial node locations for near equatorial circular satellite orbits". *Celestial Mechanics* 8 (1973) p 45-73
- [9] Rosengren, A. "Long-term Dynamics and stability of GEO orbits: the primacy of the Laplace plane". AAS 13-865
- [10] Lamy, A. et al "Selection and optimization of a constellation of satellites for continuous zonal coverage". ISSFD 2009
- [11] Lamy, A. et al "Resonance Effects on Lifetime of Low Earth Orbit Satellites". ISSFD 2012
- [12] Fraysse, H. et al "Statistical methods to address the compliance of GTO with the French Space Operations Act". IAC, 2013.